Fracture stress-reflecting spot relations in hot-pressed alumina

Earlier observations have shown that the areas of the regions of intense reflecting spots, observed at fracture origins in alumina ceramics by optical microscopy, vary with fracture stress [1–5]. In weak specimens the areas are relatively large and in strong specimens they are relatively small.

The reflecting spots are caused by areas of transgranular fracture [2, 6]. The fraction of transgranular fracture diminishes gradually with distance from the fracture origin [6, 7] but the eye discerns a fairly definite boundary of reflecting spots. In members, uniformly stressed in tension, the stress intensity factor (K_I), at various points on the boundary of a semi-elliptical surface crack perpendicular to the stress (σ) is [8]

$$K_I = \frac{Y\sigma}{\phi}\left(\frac{a}{c}\right)^{1/2}(a^2\cos^2\theta + c^2\sin^2\theta)^{1/4}, \quad (1)$$

in which a and c are the semi-axes of the crack as indicated in Fig. 1a and b, θ is the angle between the c-axis and a line joining the centre of the ellipse with the point on the boundary for which K_I is calculated, ϕ is the elliptic integral having the form

$$\phi_1 = \int_0^{\pi/2}\left[1-\left(1-\frac{a^2}{c^2}\right)\sin^2\theta\right]^{1/2} d\theta, a \leqslant c \quad (2)$$

$$\phi_2 = \frac{a}{c}\int_0^{\pi/2}\left[1-\left(1-\frac{c^2}{a^2}\right)\sin^2\theta\right]^{1/2} d\theta, c \leqslant a \quad (3)$$

so that $\phi_2 = (a/c)\phi_1$ for a given eccentricity of the ellipse and Y is a geometrical factor that accounts for the location of the crack, surface or internal, and the size of the crack relative to the stressed member. The maxima in K_I occur at the intersections of the minor axes with the elliptical boundaries. The minima in K_I occur at the intersections of the major axes with the elliptical boundaries. We are mainly interested in the maximum values of K_I which occur at the points labelled x in Fig. 1a and b. Hence, we can compute these maximum values using

$$K_{I,max} = \frac{Y\sigma}{\phi_1}\sqrt{a} \quad \text{for } c > a \quad (4)$$

and

$$K_{I,max} = \frac{Y\sigma}{\phi_1}\sqrt{c} \quad \text{for } a > c. \quad (5)$$

The sizes of critical flaws are related to the fracture stress (σ_f) by expressions that are similar in form to Equations 4 and 5 above in which $K_{I,max}$ is equal to the critical stress intensity factor (K_{IC}) which K_{IC} is a material property. In addition, other fracture characteristics such as the locations of the mirror-mist and crack-branching boundaries in glass are known to occur at particular values of stress intensity factor [9, 10]. These, together with the qualitative observations of variations in reflecting spots referred to above raised the question whether or not the location of the reflecting spot boundary is related to σ_f by similar equations. Therefore, a and c of the reflecting spot area were measured from photographs of a number of hot-pressed (HP) alumina specimens, 3.3 mm diameter, fractured in flexure from surface fracture origins in regular strength tests and by delayed fracture. The detailed procedures were described previously [3, 4]. Although the applied stress field was non-uniform, the variation in stress across the reflecting spot region was negligible (less than about 10%).

If the flaw severity is defined as the square root of the length of the minor semi-axis divided by ϕ_1, it is a measure of the greatest stress intensification at a crack. Rearranging Equation 5 and taking the logarithm of the terms yields

$$\log\frac{K_I}{Y} = \log\sigma + \frac{1}{2}\log\frac{C}{\phi_1^2}. \quad (6)$$

Therefore, if we assume that there is a particular maximum value of the stress intensity factor, say K_R, at which the reflecting spot boundary forms along the minor axis, a plot of the fracture stress (σ_f) versus the flaw severity squared should have a slope of $-\frac{1}{2}$. Such a plot for HP alumina specimens fractured in flexure is given in Fig. 2. Values of ϕ_1 were taken from mathematical tables. A dashed line with a slope of $-\frac{1}{2}$ has been drawn

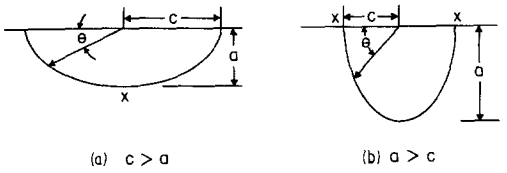

Figure 1 Semi-elliptical surface flaws.

0022–2461/80/051319–03$02.30/0

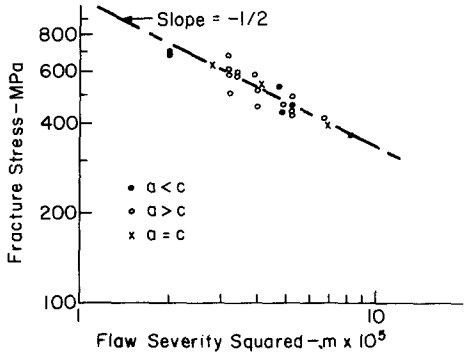

Figure 2 Fracture stress versus flaw severity squared for reflecting spot boundaries in HP alumina fractured in flexure at room temperature.

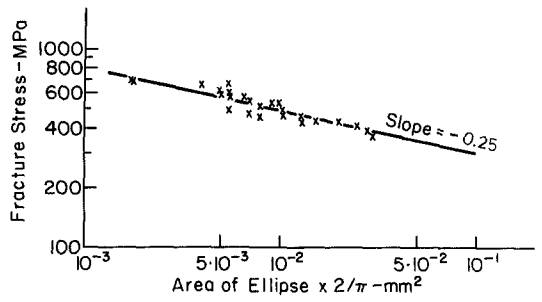

Figure 3 Fracture stress versus area of ellipse × $2/\pi$ formed by reflecting spot boundaries in HP alumina fractured in flexure at room temperature.

through the data. Clearly, the slope indicated by the data is close to $-\frac{1}{2}$. K_R was estimated at a value of C/ϕ_1^2 of 4.5×10^{-5} m, using $Y = 2.0$ for surface cracks yielding $K_R = 6.6\,\mathrm{MPam}^{1/2}$. The critical stress intensity factor (K_{IC}) of a similar alumina body was measured by Bansal and Duckworth [11] and found to be $4.2\,\mathrm{MPam}^{1/2}$. Therefore, K_R is substantially greater than K_{IC} showing that the reflecting spot boundary is not the subcritical crack growth boundary.

The average value of the stress intensity factor at the intersection of the major axis with the boundary of the reflecting spots ($K_{I,min}$) was calculated yielding $5.5\,\mathrm{MPam}^{1/2}$. This value is also greater than K_{IC}. The variation in K_I along the reflecting spot boundary is substantial and is clearly different from the constant values of K_I observed along crack-branching boundaries [9, 10]. This observation points out a contradiction involved in characterizing the area of reflecting spots as the "inner mirror" [5]; that is, as analogous to the region inside the mirror-mist boundary in glass. If the area of reflecting spots were associated with crack branching as implied by this characterization, K_I should be constant around the boundary [10].

Bansal [8] has shown that the areas of critical flaws (A) are related to the fracture stress by

$$\sigma_f \cong \frac{1.68}{Y}\frac{K_{IC}}{A^{1/4}}. \qquad (6)$$

By analogy, one might expect a similar relation to hold for the areas of ellipses formed by reflecting spot boundaries. The area of an ellipse is πac so that for a semi-ellipse $(2/\pi)A = ac$. The log of σ_f is plotted versus $\log(2/\pi)A$ in Fig. 3. The slope is $-\frac{1}{4}$, as expected.

The results for delayed fracture specimens were analysed similarly. The average K_R calculated at the minor axis intersections was $6.6\,\mathrm{MPam}^{1/2}$, confirming the above result and showing that the observed increase in the area of the reflecting spots in delayed fracture specimens is a result of the lower fracture stresses caused by subcritical crack growth rather than being a direct result of loading rate. The c-axes of the ellipses formed in delayed fracture specimens appear to be greater on the average relative to the a-axes, compared with specimens fractured using linear loading rates. This difference may have occurred as a result of stress corrosion enhanced crack growth along the surface.

In earlier work it was shown that the fracture mode, represented in this case by the percent intergranular fracture (PIF) varied with stress intensity factor along radii from fracture origins as indicated in an earlier paper [7]. Lower values of PIF indicate the presence of proportionately greater amounts of transgranular fracture (cleavage). At $K_I = 6.6\,\mathrm{MPam}^{1/2}$, the PIF is about 50%. Therefore, it appears that at magnifications of ×60, the eye preceives the reflecting spot boundary to be at about 50% transgranular fracture.

In conclusion, it has been shown that the location of the reflecting spot boundary is related to σ_f by equations similar to those normally used to calculate the stress intensity factors at the boundaries of elliptical cracks. The maximum stress intensity factor at the reflecting spot boundary is a material property with a value of about

6.6 MPam$^{1/2}$. However, the fact that the stress intensity factor is not constant along these boundaries may indicate that the reflecting spot regions are not analogous to the mirrors observed in glass fracture surfaces which are bounded by crack branching.

References

1. H. P. KIRCHNER, W. R. BUESSEM, R. M. GRUVER, D. R. PLATTS and R. E. WALKER, "Chemical Strengthening of Ceramic Materials," Ceramic Finishing Company Summary Report, Contract N00019-70-C-0418, (December, 1970).
2. H. P. KIRCHNER and R. M. GRUVER, *Phil. Mag.* 27 (1973) 1433.
3. R. M. GRUVER, W. A. SOTTER and H. P. KIRCHNER, "Fractography of Ceramics," Ceramic Finishing Company Summary Report, Contract N00019-73-C-0356 (November, 1974).
4. H. P. KIRCHNER, R. M. GRUVER and W. A. SOTTER, *Mater. Sci. Eng.* 22 (1976) 147.
5. R. W. RICE, in "Fracture Mechanics of Ceramics", Vol. 1, edited by R. C. Bradt, D. P. H. Hasselman and F. F. Lange, (Plenum, New York, 1974) pp. 323–45.
6. H. P. KIRCHNER and R. M. GRUVER, *J. Amer. Ceram. Soc.* To be published.
7. *Idem, J. Mater. Sci.* 14 (1979) 2110.
8. G. K. BANSAL, *J. Amer. Ceram. Soc.* 59 (1976) 87.
9. H. P. KIRCHNER, *Eng. Fract. Mech.* 10 (1978) 283.
10. H. P. KIRCHNER and J. W. KIRCHNER, *J. Amer. Ceram. Soc.* 62 (1979) 198.
11. G. K. BANSAL and W. H. DUCKWORTH, in "Fracture Mechanics of Ceramics", Vol. 3, edited by R. C. Bradt, D. P. H. Hasselman and F. F. Lange (Plenum, New York, 1978) pp. 189–204.

Received 23 August
and accepted 1 October 1979

H. P. KIRCHNER
D. M. RICHARD
Ceramic Finishing Company,
P.O. Box 498,
State College,
Pennsylvania 16801,
USA

The Vickers micro-hardness of non-stoichiometric niobium carbide and vanadium carbide single crystals up to 1500° C

This communication describes the micro-hardness of VC and NbC single crystals up to 1500° C and the temperature dependency of the relaxation behaviour of indentation. These results are compared with a previous study of TiC single crystals [1]. There has been some controversy [1–8] as to whether the activation energy for high-temperature deformation in transition metal monocarbides is coincident with that for the lattice diffusion of carbon, which is also clarified by the present study.

Single crystals were prepared by an *r.f.* floating zone process, in an Ar atmosphere of 3 atm, as for TiC [9, 10]. The composition of these crystals corresponds to $VC_{0.88}$ and $NbC_{0.80}$ determined by chemical analysis. The single crystals have high dislocation densities (10^6 to 10^7 cm^{-2}), which cause the generation of subgrain boundaries. The crushed samples of $NbC_{0.80}$ crystals contain a little precipitated Nb_2C confirmed by X-ray powder diffraction methods. The electrical resistivities of $VC_{0.88}$ and $NbC_{0.80}$ are 69 and 135 $\mu\Omega$ cm, respectively. The arrangement of vacancies in $VC_{0.88}$ corresponds to an ordered state judging from the behaviour of the electrical resistivity of VC_x at various vacancy concentrations, including its arrangement studied by Williams [11].

The single crystals of VC are large enough to enable the hardness on three planes to be measured, while NbC is limited to only the (1 0 0) plane because of difficulty in preparing crystals as long as VC. The experiment at room temperature was carried out using a Vickers micro-hardness tester, Akashi Seisakusho Ltd. High-temperature indentation was performed using a Nikon high-temperature micro-hardness tester Model QM[1].

Fig. 1 shows the anisotropy hardness of VC and NbC single crystals at room temperature. The hardness anisotropy is less pronounced than in TiC [1], which would be due firstly to the non-stoichiometry of the crystals and secondly to the possibility of formation of ordering of vacancies [12, 13]. The anisotropy in the (1 0 0) planes

0022–2461/80/051321–04$02.40/0